EBJ Manuscript Nr.
(will be inserted by hand later)

Calculation of IR dichroic values and order parameters from molecular dynamics simulations and their application to structure determination of lipid bilayers

Christian Bolterauer[1*] **and Helmut Heller**[2**]

[1] Technical University of Munich, Physics Department, E22, Garching, Germany.
[2] Ludwig Maximilians University, Institute for Medical Optics, Theoretical Biophysics Group, Theresienstr. 37, 80333 Munich, Germany. (phone: +49-89-2394-4565, FAX: +49-89-2394-4607)

Received: August 1, 1995 / Accepted: March 4, 1996

Abstract In polarized infrared (IR) absorption experiments, dichroic values are used to study the structure and orientation of lipid molecules. From computer simulations, we obtained angular distributions of IR transition moment (TM) orientations of the stretch vibrations of CH_2 groups of 1-palmitoyl-2-oleoyl-*sn*-glycero-3-phosphatidylcholin (POPC) lipid bilayers in the gel (L_β) and fluid (L_α) phases. From these distributions, we calculated dichroic absorption values, as well as order parameters. We established a connection between the dichroic ratio R^{ATR}, which is measured in IR-ATR setups, with the dichroic ratio D and the order parameter S_{zz}. The calculated values compare well with experimental results for the fluid phase. In addition, we computed angular distributions of transition moments with respect to the tail director orientation for the gel and the fluid phases. Only small differences were found between the distributions in the symmetric stretch orientation, the asymmetric stretch orientation, and the C–H bond orientation of CH_2 groups. The distributions of tail directors of POPC showed average tilts of 14.7^0 in the gel phase and 32.9^0 in the fluid phase. We developed a theory which makes it possible to calculate average tilt angles of tail directors in the gel phase from dichroic absorption values obtained from IR measurements for a wide range of lipids. Legendre coefficients were calculated from TM distributions. Order parameters, defined as the second Legendre polynomial, were found to closely approximate the TM distribution in lipid bilayers in the fluid phase.

Key words: IR absorption – CH2 stretch vibration – molecular director – angular distribution – 1-palmitoyl-2-oleoyl-*sn*-glycero-3-phosphatidylcholin (POPC)

* cboltera@physik.tu-muenchen.de
** heller@nirvana.imo.physik.uni-muenchen.de
Correspondence to: H. Heller

Abbreviations: IR, infrared; ATR, attenuated total reflection; TM, transition moment; MD, molecular dynamics; NMR, nuclear magnetic resonance; POPC, 1-palmitoyl-2-oleoyl-*sn*-glycero-3-phosphatidylcholin; POPG, 1-palmitoyl-2-oleoyl-*sn*-glycero-3-phosphatidylglycerol; DPPC, 1,2-dipalmitoyl-*sn*-glycero-3-phosphatidylcholin.

1 Introduction

Membranes play a central role for structure and function of living systems. Many biological membranes are formed from double layers of various amphipathic lipid molecules and contain embedded proteins and other functional units. Most experimental investigations or computer simulations, however, employ simplified model membranes, e.g., lipid bilayers of a single type of lipid.

A wide range of experimental methods, e.g., NMR (Seelig & Seelig 1980; Seelig & Macdonald 1987), neutron scattering (QENS[1]) (König *et al.* 1992), X-ray diffraction (He *et al.* 1994), electron microscopy (Bayerl *et al.* 1988), atomic force microscopy (Egger *et al.* 1990), and IR light absorption (Hübner & Mantsch 1991; Chia & Mendelsohn 1992), is being used to study structure and dynamics of membranes. Among these experimental techniques, only polarized IR absorption allows the study of dynamical processes on a picosecond time scale[2], a time scale which is easily accessible to molecular dynamics (MD) simulations. The use of IR absorption has the advantage that absorption properties can be obtained in both major phases: the fluid and the gel phase[3].

IR absorption is dependent on the angular orientation of transition moments of specific molecular group vibrations (normal modes), e.g., CH_2 stretch vibrations, and can therefore be used to probe the conformational states of the lipid molecules with respect to the polarized electrical field vectors. Because the IR absorption signal also depends on the overall orientation of the lipid tails, it is also possible to derive tail tilt angles from IR absorption measurements. From our computer simulations we determined the angular distributions of IR transition moments in the lipid tails and therefore the detailed structure of these tails.

[1] Quasi-elastic incoherent neutron scattering.
[2] The intrinsic time scale of IR absorption lies in the picosecond range; however, typical experimental setups introduce an additional averaging process in the millisecond range.
[3] Interpretation of NMR data in the gel phase is very difficult.

Theoretically, it is possible to compute *normalized* absorption coefficients from angular probability distributions of TM orientations (cf. Sec. 2.1). However, due to the lack of an appropriate reference signal, it is difficult to normalize IR absorption coefficients in experiments. This problem is circumvented in *polarized* absorption measurements. The dichroic absorption values obtained in these experiments are defined as the *fraction* of absorption in two different polarization planes (see Sec. 2.2). This alleviates the need for normalization and makes the dichroic ratio a suitable observable for comparison of experimental and simulation data.

The introduction of parallel computers with their increased computational power makes it possible to study large ensembles of molecules at atomic detail by means of MD simulations. A sufficiently large (over 25,000 atoms) and realistic (no truncation of electrostatic interactions) computer model of a POPC membrane was constructed and simulated over several hundred picoseconds (Heller *et al.* 1993). The macroscopic observables, e.g., the IR dichroic ratios and order parameters, can then be computed by averaging the microscopic data over an appropriate range of time and space. The microscopic data obtained in the computer simulation give us a deeper insight into the structure and dynamics of membranes than the experimental data alone would allow.

In the following two sections we outline the theory of IR absorption and detail how to derive the experimental observables D, R^{ATR}, and S_{zz}^{IR} from MD simulations. In the Results section we first show that the important requirement of azimuthal symmetry of the TM distribution is fulfilled. For both phases we then investigate the tilt of the tail directors and differences of the TM distributions between the lab and lipid coordinate system. Comparison of the observables D, R^{ATR}, and S_{zz}^{IR} computed from our MD simulations with experimental results shows good agreement. From our simulation data we derive a general, empirical relationship between the dichroic ratio D and the average tilt angle γ. This model distribution and the theory we developed in Sec. 3.3 make it possible to now calculate average tilt angles of tail directors in the gel phase from dichroic absorption values for a wide range of lipids. To test the widely used concept of a single order parameter, we expand the TM distribution in a Legendre series and compute Legendre coefficients up to the 10^{th} order, which are found to rapidly converge towards zero.

2 Theory

In order to compute the experimentally accessible IR properties from MD simulations, we will first summarize the theory of IR absorption in lipid membranes and then explain the experimental setup used in IR-ATR experiments.

2.1 IR-Absorption

In the normal mode approximation used in infrared vibrational spectroscopy, the quantum state of a molecule is decomposed into an ensemble of uncoupled harmonic dipolar oscillators, called normal modes. Each normal mode is described by a normal coordinate Q and an associated oscillating dipole moment $(\partial\boldsymbol{\mu}/\partial Q)$, called transition moment (TM). Normal modes describe specific group-vibrations, which are characterized by their absorption frequencies in an IR spectrum (Bellamy 1975; Snyder & Schachtenschneider 1963). In the IR-limit, the wave length of the radiation field ($\lambda \approx 10\,\mu$m $= 10^5$ Å) is large in comparison to molecular group dimensions ($d \approx 10$ Å). The basic equation of IR absorption (Heitler 1954) of an ensemble of (uncoupled) molecular vibrations can be written as (Fringeli & Gunthard 1981)

$$I_{Absorb} = \int_V d\mathbf{r} \quad C(\mathbf{r}) \; \left| \left(\frac{\partial \boldsymbol{\mu}}{\partial Q} \right)(\mathbf{r}) \right|^2 \\ |\mathbf{E}(\mathbf{r})|^2 \;\; \cos^2\left(\mathbf{E}(\mathbf{r}), \left(\frac{\partial \boldsymbol{\mu}}{\partial Q} \right)(\mathbf{r}) \right) \; . \quad (1)$$

We integrate over the volume V of the sample to take all vibrational groups into account. $C(\mathbf{r})$ contains all constants of the normal mode. $\mathbf{E}(\mathbf{r})$ denotes the polarized electrical field vector of the incident IR beam. For a weakly absorbing thin film (e.g., lipid bilayers), polarization direction and the amplitude of the electrical radiation field $|\mathbf{E}(\mathbf{r})|$ can be assumed to be constant over the sample volume V. If the oscillator strength of a specific normal mode $C \cdot \left| \left(\frac{\partial \mu}{\partial Q} \right) \right|^2$ is independent of the position in the sample, the absorption will depend only on the orientation of the TMs with respect to the polarization direction. Therefore, it is not possible to resolve the position of TMs with IR absorption. Thus, we describe the ensemble of TMs by an angular probability distribution of TM orientations, $f(\theta, \varphi)$, which is most adequately expressed in spherical coordinates. If TMs change their direction significantly during the typical IR absorption time scale of picoseconds, $f(\theta, \varphi)$ will also include a time average.

Figure 1 introduces the nomenclature used in this paper. Without loss of generality, we first assume the IR beam to be polarized in z-direction ($\alpha = 0^o$, $\beta = 0^o$). Then we get for the normalized absorption coefficient A_z

$$A_z = \frac{I_{Absorb}}{N \; |\mathbf{E}|^2 \; C \; \left| \left(\frac{\partial \mu}{\partial Q} \right) \right|^2} \\ = \int_0^{2\pi} d\varphi \int_0^{\pi} d\theta \sin(\theta) \; \cos^2(\theta) \; f(\theta, \varphi) \; . \quad (2)$$

N is the number of illuminated TMs, θ denotes the azimuth angle between the $\mathbf{E}$-field vector and the TM direction of the normal mode and φ is the rotation angle around the z-axis (cf. Fig. 1).

To calculate the absorption coefficient A for an arbitrary polarization direction (α, β) we have to replace the cosine in Eq. (2) by a generalized expression. A coordinate transformation (see App. A) of the unit spherical z-component $z = \cos(\theta) \rightarrow Z$ in the new direction (α, β) can be written as

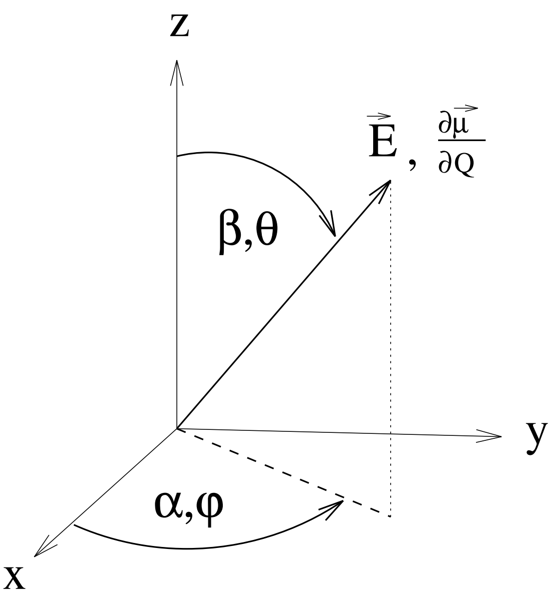

Figure 1. Definition of the coordinate system used in this paper: The solid angles, α, β denote the orientation of the polarized electrical field $\mathbf{E}$. The angles θ, φ denote the orientation of the transition moment $(\partial\boldsymbol{\mu}/\partial Q)$. The angular distribution of transition moment orientations is thus a function of θ, φ.

$$
\begin{aligned}
Z(\alpha,\beta,\theta,\varphi) = \;& \cos(\alpha)\ \sin(\beta)\ \cos(\varphi)\ \sin(\theta)\ + \\
& \sin(\alpha)\ \sin(\beta)\ \sin(\varphi)\ \sin(\theta) + \\
& \cos(\beta)\ \cos(\theta)\ . \qquad (3)
\end{aligned}
$$

The absorption coefficient in an arbitrary direction (α, β) then becomes

$$A(\alpha,\beta) = \int_0^{2\pi} d\varphi \int_0^{\pi} d\theta \sin(\theta)\, Z^2(\alpha,\beta,\theta,\varphi)\, f(\theta,\varphi)\ . \qquad (4)$$

In many systems, e.g., homogeneous lipid membranes, $f(\theta, \varphi)$ shows rotational symmetry around some symmetry axis z_s. Without loss of generality, we assume $z_s \equiv z$. In this case, $f(\theta, \varphi)$ can be described by the azimuth angle θ alone. Integration of Eq. (4) over φ then yields

$$A(\beta) = \int_0^{\pi} d\theta \sin(\theta)\, \tilde{Z}^2(\beta,\theta)\, \tilde{f}(\theta), \quad \tilde{f}(\theta) = 2\pi f(\theta)\ , \qquad (5)$$

with

$$\tilde{Z}^2(\beta,\theta) = \cos^2(\beta)\ \cos^2(\theta) + \frac{1}{2}\sin^2(\beta)\ \sin^2(\theta)\ . \qquad (6)$$

From Eq. (6), it follows that $\tilde{Z}^2$ decomposes in just two quadratic terms. The first term is the component of the squared directional cosine $(\tilde{Z}^2)$ in z-direction and the second term is the component in the x, y-plane. This decomposition allows us to compute the ratio of the IR absorption in two polarization directions, the dichroic ratio.

2.2 Dichroic Ratio

Due to the lack of an appropriate reference signal, it is experimentally difficult to determine the absolute absorption coefficient A. In systems with azimuthal symmetry, e.g., homogeneous lipid bilayers, the dichroic ratio D is used as an observable instead. It is defined as the fraction of two absorption coefficients A in two perpendicular polarization directions

$$D = \frac{A_{\parallel}}{A_{\perp}}\ , \qquad (7)$$

where $A_{\parallel}$ is the absorption coefficient for IR radiation polarized parallel to the symmetry axis z of the TM distribution and $A_{\perp}$ is the absorption coefficient for IR radiation polarized perpendicular to the symmetry axis z. We then get for the relative absorption coefficients, $A_{\parallel}$ and $A_{\perp}$, using Eqs. (5, 6) with $\beta = 0$ ($\beta = 90^0$) parallel (perpendicular) to z

$$A_{\parallel} = \int_0^{\pi} d\theta \sin(\theta)\ \cos^2(\theta)\ \tilde{f}(\theta)\ , \qquad (8)$$

$$A_{\perp} = \frac{1}{2} \int_0^{\pi} d\theta \sin(\theta)\ \sin^2(\theta)\ \tilde{f}(\theta)\ . \qquad (9)$$

The factor $\frac{1}{2}$ is a consequence of the disc shape of the distribution in the x, y-plane. D varies from 0 to ∞ and yields unity, if the distribution is isotropic. The values for totally oriented TMs also vary from 0 to ∞ depending on the orientation angle θ of the TMs with respect to the symmetry axis z.

In the experiment the dichroic ratio D is measured. From our computer simulation we can obtain $\tilde{f}(\theta)$ and calculate the dichroic ratio D, which can be compared to the experiment. Thus we can derive information about the conformation of the lipids from IR measurements together with computer simulations.

2.3 Dichroic Ratio in IR-ATR Experiments

Figure 2 shows a typical experimental attenuated total reflection (ATR) setup. A lipid membrane is attached to the crystal on the top face (see inset in Fig. 2). The IR light beam enters the ATR crystal through its left face and exits the crystal after many total reflections through the right face (only three reflections are shown). The total internal reflection of the IR light beam inside the ATR crystal results in exponentially decaying evanescent electrical fields $\mathbf{E}$, as light penetrates into the optically less dense lipid membrane. For a thin membrane ($d \ll \lambda$) the decay in the membrane can be neglected. The lipids absorb energy from the light beam and that attenuation is detected. On an ATR crystal the lab coordinate system is defined as shown in Fig. 2. The electrical evanescent field component $E_{\parallel}^{\beta}$ for an incident IR beam polarized parallel to the z-axis is tilted away from the z-axis by an angle β. Therefore, a dichroic ratio definition different

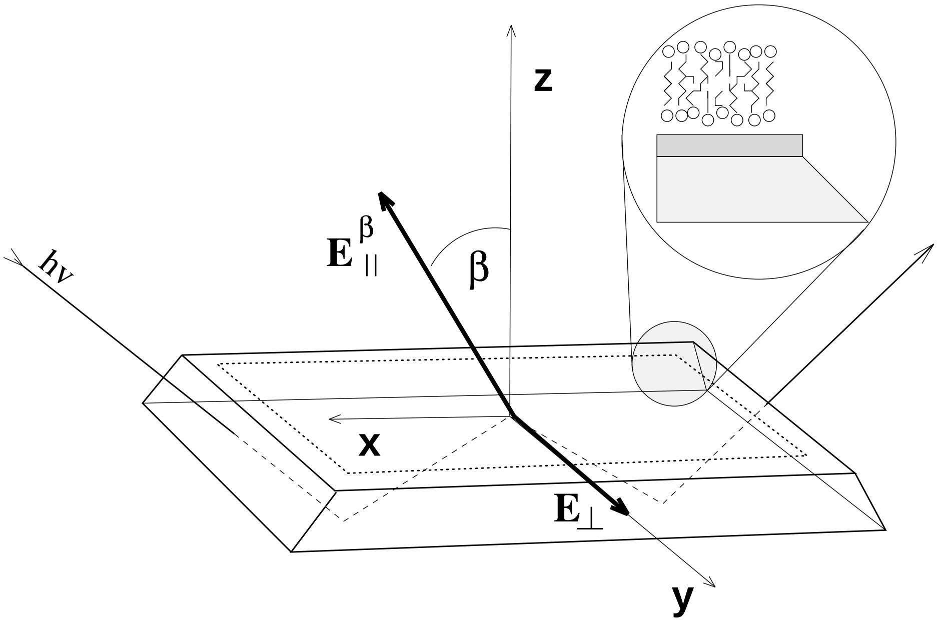

Figure 2. Experimental attenuated total reflection (ATR) setup: shown is an ATR crystal (e.g., germanium or silicon). On the top face a lipid membrane is attached to the crystal. A thin layer of solvent (usually water, shown in dark grey in the inset) can be found between the ATR crystal and the lipids. IR light enters the crystal from the left and its intensity is measured (not shown) after it has left the crystal. The total internal reflection of the IR light beam inside the ATR crystal results in exponentially decaying evanescent electrical fields $\mathbf{E}$, as light penetrates into the optically less dense lipid membrane. For a thin film ($d \ll \lambda$) the decay in the film can be neglected. On the surface of the crystal the parallel polarized component $E_{\|}^{\beta}$ is tilted (Harrick & Pre 1966) by an angle β in the x,z-plane. The perpendicular polarized component $E_\perp$ is oriented parallel to the y-axis.

from the one given in Eq. (8) is used in IR-ATR experiments. Using Eqs. (5, 9) the experimental dichroic ratio R^{ATR} is defined as

$$R^{ATR}(\beta) = \frac{E_z^2 + E_x^2}{E_y^2} \cdot \frac{A_{\|}(\beta)}{A_\perp} \; . \tag{10}$$

The evanescent field components E_z, E_x, E_y are dependent on the internal reflection angle in the crystal and are defined as

$$E_z = E_{\|}^{\beta} \; \cos(\beta) \tag{11}$$

$$E_x = E_{\|}^{\beta} \; \sin(\beta) \tag{12}$$

$$E_y = E_\perp \; . \tag{13}$$

The electrical field components E_i in the film are usually complicated functions of the refraction indices of bulk media (e.g., water) between the ATR crystal and the film and the refraction index of the film. They are usually calculated with the equations given by Harrick (Harrick & Pre 1966). Inserting Eqs. (7–9) into Eq. (10) and using Eq. (11–13), the dichroic value D can be computed from the dichroic ratio R^{ATR} by

$$D = \frac{E_y^2 \; R^{ATR} - E_x^2}{E_z^2} \; . \tag{14}$$

Note that this relationship between D and R^{ATR} only holds in case of azimuthal symmetry of the TM distribution. In Sec. 4.1 we will show that this symmetry is given in our case.

2.4 Order Parameter

To allow comparisons of IR data with NMR data, we define the IR order parameter S_{zz}^{IR} similar to the NMR order parameter S_{zz}^{NMR}. The order parameter S_{zz} measures the degree of orientation of the TMs with respect to the z-axis. It is defined by a time and ensemble average

$$S_{zz} = \frac{3}{2} \int_0^{2\pi} d\varphi \int_0^{\pi} d\theta \sin(\theta) \; f(\theta,\varphi) \; \cos^2(\theta) - \frac{1}{2} \; , \tag{15}$$

where the time average is already included in $f(\theta,\varphi)$. Inserting Eq. (2) into Eq. (15) gives for the infrared order parameter S_{zz}^{IR}

$$S_{zz}^{IR} = \frac{3}{2} \; A_z \; - \frac{1}{2} \; . \tag{16}$$

Using the definition of the dichroic ratio Eq. (7) and the appropriate absorption coefficients we get

$$S_{zz} = \frac{3}{2} \cdot \frac{D}{D+2} - \frac{1}{2} \; . \tag{17}$$

For a detailed derivation and discussion see (Bolterauer 1996).

3 Methods

In this section we will introduce the simulation method, motivate the use of a local *molecular* coordinate system, and show how to derive IR observables from MD simulation data.

3.1 Molecular Dynamics Simulation

Computer simulations of biological macromolecules are based on a classical mechanical model of biomolecules. For the nuclei of the N atoms of a molecule the Newtonian equations of motion

$$m_i \frac{d^2}{dt^2}\mathbf{r}_i \;=\; -\nabla_i E(\mathbf{r}_1, \mathbf{r}_2, \ldots, \mathbf{r}_N) \;, \quad i = 1, 2, \ldots N \quad (18)$$

are assumed to hold. $\mathbf{r}_i$ denotes the position of the i-th atom and m_i its mass. We have used the notation $\nabla_i = \partial/\partial\mathbf{r}_i$. Different types of forces act on the atoms in the molecular assembly. These contributions are approximated by the semi-empirical energy function E, the total potential energy of simulated molecules. These forces and the method of molecular dynamics simulation has been described in detail elsewhere (Heller *et al.* 1990; Grubmüller *et al.* 1991; Heller 1993). The primary result of a molecular dynamics simulation is a complete set of coordinates for all atoms stored at regular time intervals[4]. The sum of all coordinate sets is called a trajectory. This detailed information allows one to compute macroscopic observables through averaging over time and space. Ideally, the averages stretch over time and space ranges similar to those of real lab experiments, i.e., milliseconds and millimeters in IR-absorption studies.

In the present work, we simulated a POPC bilayer with 200 POPC lipids and over 5,000 water molecules, totaling 25,000 atoms, for well over 300 ps. We used the parallel molecular dynamics program EGO (Heller 1988; Heller *et al.* 1990; Banko & Heller 1991; Sinha *et al.* 1994). EGO[5] is written in C, runs on many platforms, e.g., the CRAY T3D, clusters of workstations under PVM, on powerXplorer-systems under PARIX, and on Transputer systems, and achieves a speed almost proportional to the number of nodes. The program is input/output-compatible with CHARMm(Brooks *et al.* 1983) and X-PLOR(Brünger 1988; Brünger 1990). EGO employs the CHARMm force field and uses the same parameter files and protein structure files as X-PLOR. The program uses a modified Verlet algorithm (Verlet 1967) with a distance class algorithm (Grubmüller *et al.* 1991) for the non-bonded interactions, i.e., it does not truncate the Coulomb and van der Waals forces. A parallel version of the SHAKE algorithm (Ryckaert *et al.* 1977; Raine 1990) constrains the bond length for hydrogen atoms and allows an integration time step of 1 fs (Heller 1993).

The simulation data for the fluid phase of POPC have been taken from a previous work of one author (Heller *et al.* 1993; Heller 1993) and are described in detail there. New simulations were performed for the gel phase on a 16 node parallel computer, a powerXplorer from the German company Parsytec. To this end the short (55 ps) gel phase simulation of (Heller *et al.* 1993) was taken as a starting point and continued for 70 ps to achieve equally long simulation times of 120 ps for gel and fluid phase, each. The final 38 ps of each simulation run (gel and fluid) were used for time averaging. Sample averages were formed from all unrestrained[6] lipids only; the atomic positions were sampled every 100 fs.

[4] 128 fs in the present case.

[5] EGO is available by ftp from URL ftp://ftp.imo.physik.uni-muenchen.de/pub/ego/ego_viii.taz. Sample membrane coordinates can be downloaded from the same site.

3.2 Molecular Directors and Molecular Coordinates

To study orientational order in lipid films, it is useful to distinguish between the orientational order of lipids in a membrane and the orientational order of TMs *within* a lipid molecule. The orientation of a lipid in a membrane is measured using its molecular director, which is commonly defined by the mean orientation of the lipid tails. Depending on the averaging process of the experimental technique (e.g., NMR, IR), different definitions of molecular directors are used. In IR experiments, the molecular director is defined by the main optical axis, i.e., the principal axis of the TM distribution.

Based on the computer simulated microscopic data, we defined the two tail directors as the vectors between the carbonyl carbon and the methyl carbon of each lipid tail (thick black lines in Fig. 3). To describe the TM orientations in *lipid coordinates*, we defined a new $\widehat{z}$-axis[7] for each lipid tail using the direction of its tail director. Without loss of generality, the projection of the orientation of the glycero-group perpendicular to the new $\widehat{z}$-axis defines the new $\widehat{x}$-axis. The vector product of these two new axes gives the orientation of the new $\widehat{y}$-axis.

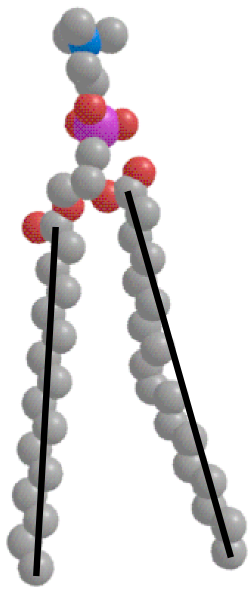

Figure 3. Definition of the tail director used in the subsequent analysis. The black lines indicate the tail directors for each lipid tail, namely the vector between the carbonyl carbon and the methyl carbon of each lipid tail.

[6] To maintain the shape of the membrane patch, 51 lipids were positionally restrained; for details of the simulation see (Heller *et al.* 1993).

[7] We use a $\widehat{\ }$ to distinguish the lipid from the lab coordinate system.

3.3 Dependence of Dichroic Values on Director Tilts in the Gel Phase

It is a well-documented observation (Zaccai *et al.* 1979; Small 1986; Damodaran *et al.* 1992) that in the gel phase, the lipid tails show a high degree of orientation; only a few gauche kinks occur. Molecular directors of different kinds of lipids, e.g., POPC, DPPC, DMPC, show different characteristic mean tilt angles γ when measured against the membrane normal. Because the TM distributions in the gel phase are highly oriented for many types of lipids, we assume that the TM distributions of those lipids, measured in respect to *lipid*-coordinates, are comparable[8]. The distribution of TM orientations for POPC in the lipid coordinate system, $\widehat{\tilde{f}}(\theta)$, derived from our MD simulation, can then serve as a model distribution for other lipids.

For POPC, we can show that both, the tail director and the TM distribution, have azimuthal symmetry and can be expressed as a function of a single tilt angle θ. We assume this is also true for other lipids.

The tail directors in the gel phase are arranged around a tilt angle, γ, with respect to the membrane normal, characteristic for the lipid system. Because the tail director distribution is rather narrow in the *gel* phase, we approximate it as two delta distributions (one for each layer of the membrane) at the characteristic tilt angle γ. We can then generate the distribution $\tilde{f}_\gamma(\theta)$ of TM orientations in the lab coordinate system through convolution of the model distribution with the delta distributions, thus we obtain

$$\begin{aligned}\tilde{f}_\gamma(\theta) &= \frac{1}{2}\int d\vartheta\ \Big[\delta(\vartheta-(\theta-\gamma))+ \\ &\qquad \delta(\vartheta-(\theta-(\pi-\gamma)))\Big]\ \widehat{\tilde{f}}(\vartheta) \qquad (19)\\ &= \frac{1}{2}\left(\widehat{\tilde{f}}(\theta-(\pi-\gamma))+\widehat{\tilde{f}}(\theta-\gamma)\right) \quad .\end{aligned}$$

From the distribution $\tilde{f}_\gamma(\theta)$ in the lab coordinate system, the dichroic ratio $D_{sim}(\gamma)$ as a function of γ can be computed using Eqs. (7, 8, 9). To derive the characteristic tilt angle γ for lipids other than POPC through a measurement of the dichroic ratio D_{exp} for that lipid, we set $D_{exp} = D_{sim}(\gamma)$. γ is easily obtained graphically or by an iterative numerical procedure.

3.4 Computation of IR-Absorption from MD Data

To calculate the IR absorption coefficients [using Eqs. (4, 5, 8, 9)], the angular distributions of dipolar TMs in respect to the electric field have to be derived from MD simulations as histograms of the respective angles (TM orientation or tail director orientation). For all distributions, we used a step size of 1^o as discretization for the azimuth angle θ and counted the number of TMs or tail directors found in the interval $[\theta, \theta+1^o]$ during the sampling interval of 38 ps. Sampling was performed every 100 fs over all unrestrained lipids.

[8] Nevertheless, conformational differences for unsaturated and saturated chains and the effect of different chain length may have to be considered. Although we can show that conformational differences exist, we could not find significant differences when comparing TM distributions of saturated chains with unsaturated chains in our simulation (see Results).

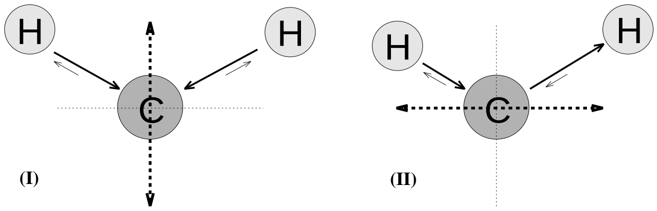

Figure 4. The symmetric (I) and asymmetric (II) CH_2 stretching modes. Only the H–C–H plane is shown. The bold, dashed double arrows mark the transition moment direction, while the thin arrows indicate the movement of the H atoms.

It is appropriate to calculate the IR absorption by averaging the ensemble of extracted TM orientations over a time span of a picosecond, the time scale of IR absorption for the observed TMs in lipid bilayers. We could not find significant differences in the TM distributions obtained for different time spans of a picosecond. Therefore, we assume that the system is ergodic for fast processes like IR absorption. Hence, we averaged over the final 38 ps of each simulation run to improve the statistics of the TM distributions.

In the MD simulation, the apolar hydrogen atoms were implicitly represented as compound atoms to keep the computational effort manageable. The orientation of the hydrogen bonds was generated after the simulation from the coordinate sets of the fatty acid carbon atoms, assuming the ideal tetrahedral geometry. This excludes the study of actual CH_2 group vibrations but still allows us to predict the major conformational state of a lipid molecule, e.g., the orientation of CH_2 groups.

Figure 4 illustrates the orientation of the TMs of CH_2 groups. According to Bellamy (Bellamy 1975), the TM for the symmetric stretch vibration is oriented parallel to the bisector of the H–C–H angle and the TM for the asymmetric stretch vibration is oriented perpendicular to the bisector of the H–C–H angle. To make a comparison to NMR experiments possible, we also investigated the orientations of C–H bonds.

4 Results and Discussion

4.1 Axial Symmetry

The basic prerequisite to calculate or measure dichroic values D is azimuthal symmetry of the TM distributions. Figure 5 shows the high axial symmetry of the various distributions from the MD simulations in the gel and fluid phases. For the fluid phase this is also in qualitative agreement with NMR measurements (Seelig 1977). Nevertheless, a small discrepancy from the ideal rotation symmetry is noticeable. The snake-shape of the contour plot Fig. 6, derived from the histogram of angular TM orientations, indicates a small tilt of the main principal axis of the distributions. The small but noticeable asym-

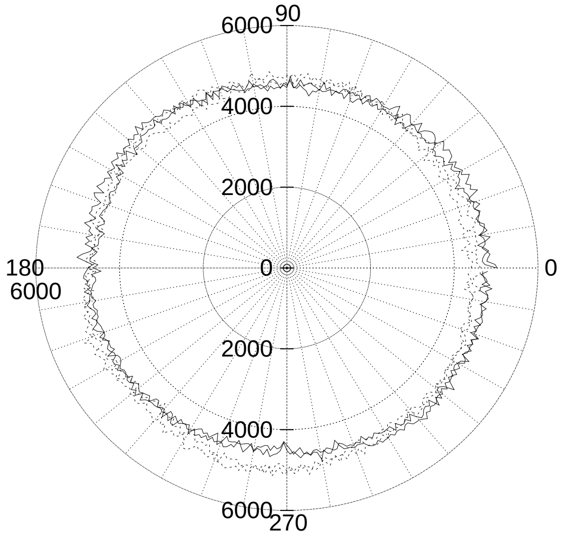

Figure 5. Distributions of transition moments in the x, y-plane. Plotted are the counts for φ angles of H–H orientations of CH_2 groups (asymmetric stretch vibration) in the lab coordinate system (solid line) and the φ angles between the tail director and the lab coordinate system (dashed line). The φ angles between the molecular and the lab coordinate systems mainly describe the orientation of the glycero-group of the lipid molecules. The plots of the fluid phase and the gel phase of POPC show no significant differences.

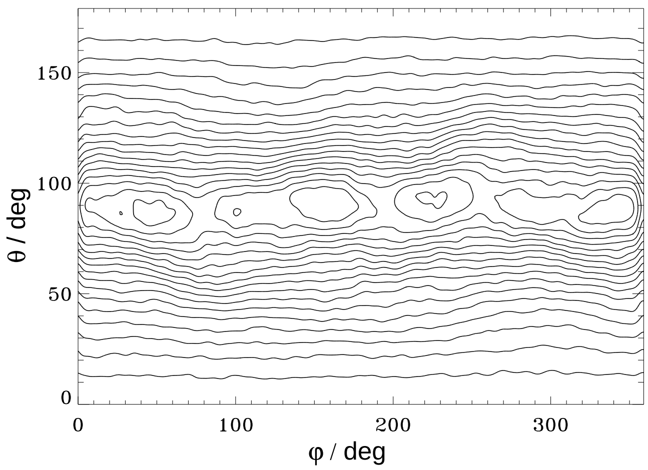

Figure 6. Contour plot of the histogram of the distribution, $f(\theta, \varphi)$, of C–H orientations. For ideal azimuthal symmetry no dependence on φ should be noticeable. The snake shape of contour lines result from a small asymmetry of the distribution of the simulated bilayer. The principal axis of the distribution is tilted against the membrane normal by a small angle.

metries of the distributions shown in Figs. 8–10 result mainly from this general tilt.

4.2 Tail Director Analysis

To determine the degree of orientation of lipid molecules in the bilayer, we calculated the distribution of tail directors. This tail director analysis can also help to clarify whether the TM distributions of CH_2 groups are determined mainly by the tail director orientations or by the internal conformational states, e.g., gauche kinks. Using Eq. (15) we calculated director order parameters S_{zz}^{tail} from the distributions of tail directors plotted for the gel phase in Fig. 7 and the fluid phase in Fig. 8. The values

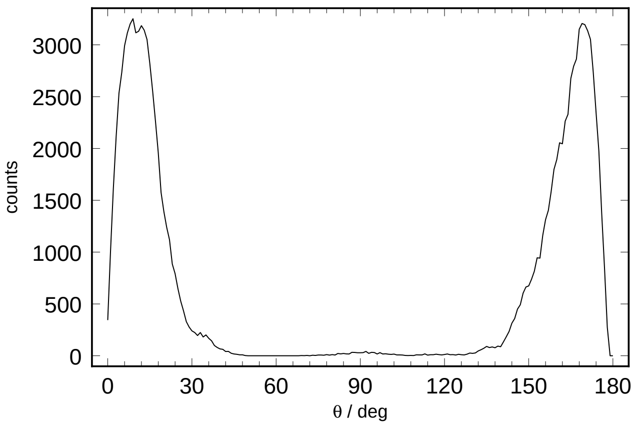

Figure 7. Angular distribution of tail directors in respect to the bilayer normal in the gel phase state of POPC.

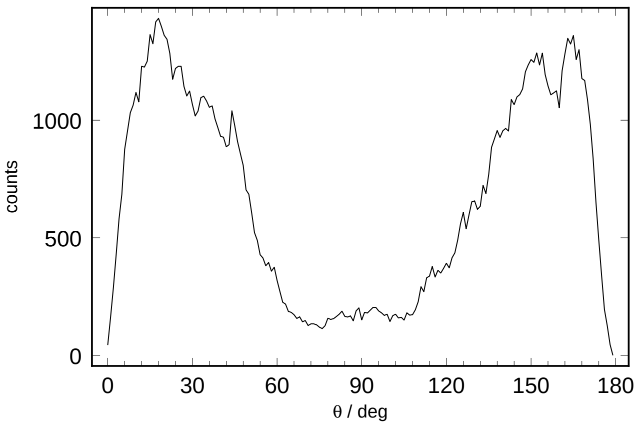

Figure 8. Angular distribution of tail directors in respect to the bilayer normal in the fluid phase state of POPC.

we obtained are $S_{zz}^{tail}(gel) = 0.786$, $S_{zz}^{tail}(fluid) = 0.323$.

From the distributions of tail directors, with respect to the bilayer normal, Figs. 7 and 8, we calculated mean tilt angles of 14.7^0 in the gel phase and 32.9^0 in the fluid phase[9]. The tail director distribution in the fluid phase is broader, which indicates that more conformational degrees of freedom (gauche defects) are excited, leading to many different director tilt angles. The strongly peaked structure of Fig. 7 suggests that only a few conformational states contribute to the director tilts.

We examined in Fig. 9 the number of gauche conformations found along the two fatty acid tails. As expected, the graphs for the gel state (filled symbols) show fewer gauche conformations than those of the fluid phase. Due to the tight packing in the gel phase only a few

[9] The tilt in the gel phase has been limited by the rigid boundary condition employed in that simulation. For details see (Heller *et al.* 1993).

[10] The original data exhibit a strong even-odd effect, which will be described in more detail in a forthcoming paper.

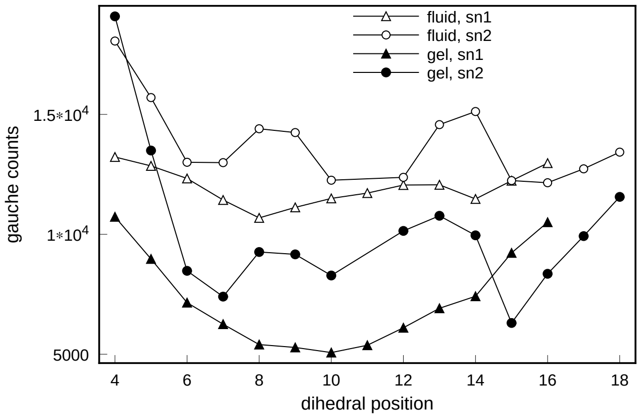

Figure 9. Number of gauche conformations along the fatty acid tails of POPC, slightly smoothed[10](the solid lines are intended as a visual guide). The gauche conformations are counted over all 200 lipids and 300 snapshots at intervals of 128 fs during the last 38 ps of the gel and fluid simulations. The dihedral angles are numbered starting at the backbone end of the tail, with increasing numbers towards the methyl end. The probability for gauche conformations is higher near the glycero-group than at the methyl end of the tail. In the fluid phase both tails, the saturated palmitoyl (triangles, *sn*1) and the unsaturated oleoyl (disks, *sn*2) fatty acid tail show a nearly constant probability from the middle of the tail (carbon no. 10) to the tail ends.

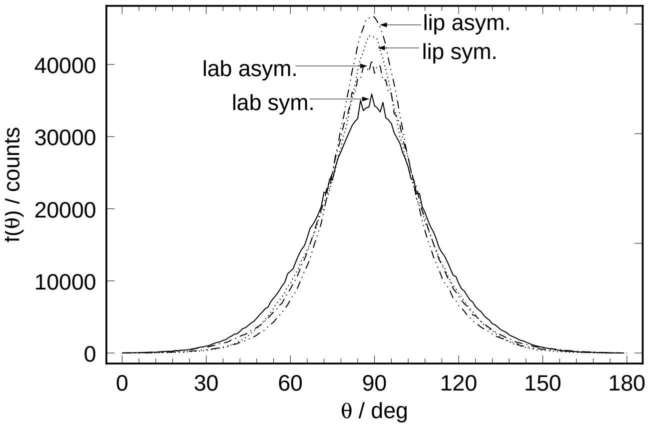

Figure 10. Angular distributions of asymmetric and symmetric CH_2 transition moment orientations in the gel phase of POPC. The obtained distributions refer to the lab z-axis and the molecular tail director system, respectively. In the gel phase the distribution of asymmetric stretch vibrations show more orientation than the symmetric stretch vibrations.

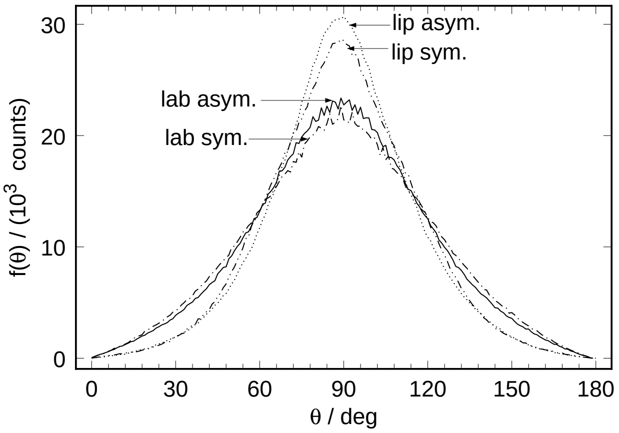

Figure 11. Angular distributions $\tilde{f}(\theta)$ of asymmetric and symmetric CH_2 transition moment orientations in the fluid phase of POPC. The obtained distributions refer to the lab z-axis and the molecular tail director system, respectively. The distribution of asymmetric stretch vibrations show more orientation than the symmetric stretch vibrations.

gauche conformations ($\approx 10\,\%$) appear in the middle of the tail, while in the fluid phase more gauche conformations ($\approx 18\,\%$) are found in the middle of the tail. This condition is especially pronounced for the saturated *sn*-1-chain.

In the fluid phase we obtained an average count of 2.76 gauche conformations per saturated *sn*-1-chain and 3.13 gauche conformations for the unsaturated *sn*-2-chain. These values are in good agreement with data from (Tuchtenhagen *et al.* 1994) for DPPC, who found 2.44 ± 0.14 gauche conformations per saturated chain for DPPC in the fluid phase. In the gel phase we found 1.69 gauche conformations per saturated *sn*-1-chain and 2.37 gauche conformations for the unsaturated *sn*-2-chain.

Gauche conformations in the middle or at the glycero-end of the chain, however, have a greater effect on the orientation of the chain director than at the methyl-end of the chain. Figure 9 shows a high probability for a gauche kink near the glycero-end of the chain. Therefore, only a few tilt angles will appear predominantly in Fig. 7. This confirms our assumption that only a few conformational states contribute to the director tilts in the gel phase.

4.3 Angular Distributions in the Lab and Lipid Coordinate System

Angular distributions $\tilde{f}(\theta)$ of CH_2 TM orientations in the lab coordinate system and in the lipid coordinate system were calculated from the MD simulation and are plotted in Fig. 10 (gel phase) and Fig. 11 (fluid phase). The distributions of the asymmetric TM orientations show a slightly higher degree of orientation than those of the TMs in the symmetric orientation. The distributions in the lab system have a spiky structure that is not observed in the corresponding distributions in the lipid coordinate system. The spikes carry over from the chain director distributions, Figs. 7 and 8, which also exhibit a spiky structure. To compare IR order parameters with NMR order parameters, we also calculated the angular distributions for C–H orientations, which are measured in NMR experiments. The distribution of C–H orientations (not shown) lies between the symmetric and asymmetric TM distributions.

Figure 10 shows that there are only small differences of the distributions for the symmetric and asymmetric TM orientation (for the definition of these orientations cf. Fig. 4), which both lie in the H–C–H plane. The same is found for the C–H bond orientations (not shown). This is to be expected for the gel phase due to the small numbers of gauche kinks and the high degree of orientation,

Table 1. Calculated dichroic values and order parameters of the asymmetric and the symmetric CH_2 TM orientations in the gel phase of POPC: The evanescent field components $E_x^2 = 1.980$, $E_y^2 = 2.198$, $E_z^2 = 0.989$ as in (Frey & Tamm 1991) were used to calculate R^{ATR}.

stretch vib.	R^{ATR}	D	S_{zz}^{IR}	ref.:
CH_2-a	0.988	0.194	-0.367	MD
CH_2-s	1.005	0.232	-0.344	MD

which leads to an alignment of most H–C–H planes parallel to the membrane plane.

In general, more gauche kinks occur in the fluid phase than in the gel phase and many H–C–H planes are tilted with respect to the membrane normal. Therefore one would expect greater differences between the symmetric and asymmetric TM distribution. It is, therefore, surprising that the distributions in Fig. 11 show only small differences for the symmetric, asymmetric, and the C–H bond orientations (the latter is not shown). This can only be understood if one takes into account the highly entropic and dynamic character of the fluid phase of lipid bilayers: a high degree of rotational and angular freedom exists. An indication of this freedom is the broadening of the TM distributions from the gel phase (cf. Fig. 10) to the fluid phase (cf. Fig. 11).

Because the symmetric/asymmetric TM distributions, which are measured in IR experiments, are almost identical to the C–H distribution, which is measured in NMR experiments, similar order parameters can be expected from IR and NMR measurements.

POPC contains two different fatty acid tails: a saturated palmitoyl tail (*sn*1) and an unsaturated oleoyl tail (*sn*2). We expected to see a difference in the TM distributions of the two tails due to the *cis* double bond in the unsaturated chain. To test this hypothesis, we calculated the angular distributions in the gel and fluid phase for the two lipid tails separately. However, we could not find any significant differences. We attribute this to the interactions of the lipid tails with those of neighboring lipids, which is the same for both tails and smoothes out individual differences.

4.4 Comparison to Experimental Data

From the angular distributions of the asymmetric stretch vibrations in the lab system plotted in Fig. 10 and Fig. 11, we calculated the dichroic values with Eqs. (7–9) and order parameters with Eq. (17) in the gel and fluid phase as $D^{gel} = 0.194$, $S_{zz}^{gel} = -0.367$ and $D^{fluid} = 0.412$, $S_{zz}^{fluid} = -0.244$. The values for perfectly oriented lipids are $D = 0$ and $S_{zz} = -0.5$. The higher orientation of the lipids in the gel phase is obvious.

Table 1 lists dichroic ratios and order parameters computed from our MD simulation of POPC in the gel phase. Experimental data in the gel phase of POPC are not accessible, because the phase transition temperature $T_c = -4^0$ C is below the freezing point of water. However, experimental data for lipids similar in structure to POPC may be compared to our calculated values for the gel phase.

Table 2. Comparison of experimental with calculated values of POPC in the fluid phase: The evanescent field components $E_x^2 = 1.980$, $E_y^2 = 2.198$, $E_z^2 = 0.989$ were used in the experiment and in the calculations. In the last section of the table the averaged NMR deuterium order parameter is shown.

stretch vib.	R^{ATR}	D	S_{zz}^{IR}	ref.:
CH_2-a	1.086	0.412	-0.244	MD
CH_2-s	1.102	0.447	-0.226	MD
CH_2-a	1.14 ± 0.21	0.534	-0.184	[11]
CH_2-s	1.07 ± 0.18	0.378	-0.262	[11]
NMR		$\overline{S_{CD}}$	$\overline{S_{zz}^{NMR}}$	ref.:
C–D		-0.122	-0.245	[12]

Table 2 lists the calculated dichroic ratios and order parameters for the fluid phase. Experimental values from (Frey & Tamm 1991) and (Seelig 1977) are also included. For the fluid phase the calculated values of D are in overall agreement with experimental data from Frey and Tamm (Frey & Tamm 1991). However, the experimental values for the asymmetric stretch vibration $D = 0.534$ ($S_{zz} = -0.184$) show less orientation, and the symmetric vibrations $D = 0.378$ ($S_{zz} = -0.262$) show more orientation than what is found in our calculations.

It has to be taken into consideration that Frey and Tamm did not study pure POPC but a mixture of POPC and POPG adsorbed to a germanium plate (cf. Fig. 2). Both the mixture of lipids and the adsorption are expected to have a distorting effect, which could explain the discrepancy between calculated and measured values.

In addition, it is possible that the symmetric CH_2 mode is influenced due to Fermi resonance with the symmetric CH_3 mode: Schachtschneider and Snyder (Schachtenschneider & Snyder 1962) suspect (for n-paraffin), "that the symmetric mode is split into two lines observed at 2,883 cm^{-1} and 2,847 cm^{-1} (for n-paraffin), by Fermi resonance with an overtone of the methylene deformation mode." Frey and Tamm observed a shoulder peak at 2,870 cm^{-1} and assign it to the the symmetric CH_3 mode. The major peak for the symmetric CH_2 mode was found to be located at 2,853 cm^{-1}. The asymmetric CH_3 mode (2,960 cm^{-1}) is further away from the asymmetric CH_2 mode (2,924 cm^{-1}) and can be resolved as a separate line. If the interaction of different modes is stronger in one polarization direction than in the other, the dichroic ratio would be altered. Therefore, absorption properties obtained from the asymmetric stretch vibration are probably more reliable for structure determination in lipids.

Comparison with Brauner et. al. (Brauner *et al.* 1987), who studied pure POPC, is difficult because we did not find their refraction index for the bulk medium, $n_3 = 1$ reasonable. We suspect that there is a water

[11] (Frey & Tamm 1991)
[12] (Seelig 1977)

layer, $n_3 = 1.33$, between the silanized germanium crystal and the lipid bilayer or if the surface is hydrophobic, a mono layer of lipids with $n_3 = 1.44$. Otherwise, the calculated values for the evanescent fields and for D are not compatible with those of Frey and Tamm. Recalculated values can be found in App. B and show the strong dependence of D and S_{zz} on the refraction index of the bulk medium. Assuming a water layer with $n_3 = 1.33$ between the lipids and the ATR crystal, we recalculated a value of $D = 0.372$ for the asymmetric CH_2 stretch vibration, which is in better agreement with Frey and Tamm (Frey & Tamm 1991) and our simulation.

4.5 Tilt of the Angular Distribution in the Gel Phase

To derive the characteristic tilt angle γ for lipids other than POPC, we used the asymmetric TM distribution in the lipid coordinate system as the model distribution and obtained D and S_{zz} using Eq. (19), as explained in Sec. 3.3. In Fig. 12 the computed values for D and S_{zz} as a function of the characteristic tilt angle γ are plotted. Comparing these values to experimentally derived values

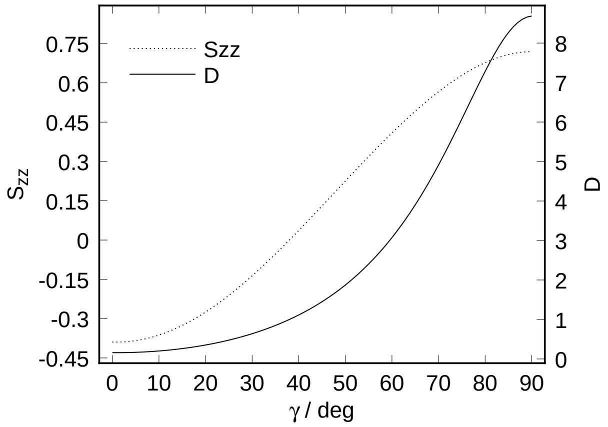

Figure 12. Dichroic values D (solid line) and order parameters S_{zz} (dotted line) are determined from the tilted model distribution in respect to the bilayer normal in the gel phase. As a model distribution the asymmetric TM distribution in the tail director coordinate system was used.

will approximate the mean tail director tilts of similar, partially unsaturated lipids in the gel phase. However, we suspect that this distribution is also applicable to saturated lipids.

4.6 Calculation of Legendre Coefficients

We tested the concept of a *single* order parameter, the averaged Legendre polynomial of second order which is used in mean field Maier-Saupe theory, by examining the higher order Legendre coefficients, which were calculated from our MD simulation.

Because the TM distributions have azimuthal symmetry, they depend on only one angle, θ, and can be expanded in a series of Legendre polynomials $P_l(cos(\theta))$

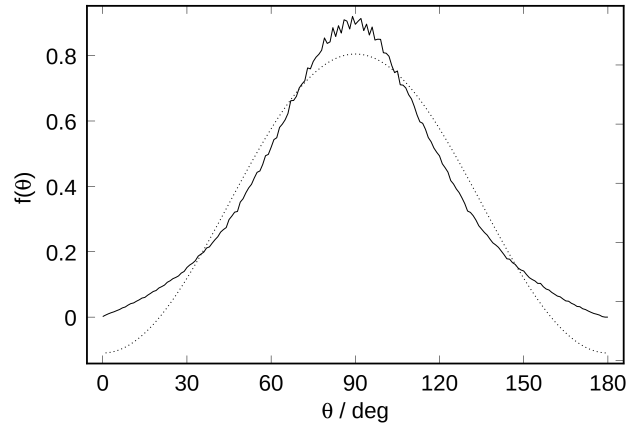

Figure 13. Comparison of the asymmetric TM distribution of POPC in the fluid phase, derived from the simulation (solid line) and with the approximated distribution (dashed line), $f_{exp}(\theta) = 0.5 - 0.610 * P_2(cos(\theta))$. The Legendre coefficient $R_2 = -0.610$ was obtained from the Legendre series of the asymmetric TM distribution (solid line); cf. Tab. 3.

Table 3. Legendre coefficients of the asymmetric TM distribution in the fluid phase of POPC (27^0C). In case of perfect bilayer symmetry the odd Legendre coefficients have to vanish.

l	0	1	2	3	4	5
R_l	0.5	0.017	-0.610	-0.022	0.186	0.013
l	6	7	8	9	10	
R_l	-0.064	-0.005	0.011	0.001	-0.013	

$$\tilde{f}(\theta) = \sum_{l=0}^{\infty} R_l \; P_l(cos(\theta)) \; ,$$
$$R_l = \frac{2l+1}{2} \int_0^{\pi} sin(\theta) \; d\theta \; \tilde{f}(\theta) \; P_l(cos(\theta)) \; . \qquad (20)$$

Only the second order Legendre polynomial can be measured in IR absorption experiments. With Eqs. (16, 17) we get

$$R_2 = \frac{5}{2}\left(\frac{3}{2}\frac{D}{(D+2)} - \frac{1}{2}\right) \quad . \qquad (21)$$

Figure 13 compares the experimentally accessible approximated asymmetric TM distribution $f(\theta) = 0.5 + R_2 \; P_2(cos(\theta))$ with the original distribution derived from the fluid simulation. The approximated distribution is in remarkably good agreement with the original distribution, although the Legendre series has been cut off after the second order.

Legendre coefficients up to 10^{th} order of the asymmetric TM distribution and the angular distribution of C–H orientations were computed from the simulation data and are listed in Tab. 3 and Tab. 4. The coefficients

Table 4. Legendre coefficients of the C–H bond distribution in the fluid phase of POPC (27^0C). In case of perfect bilayer symmetry the odd Legendre coefficients have to vanish.

l	0	1	2	3	4	5
R_l	0.5	0.015	-0.596	-0.017	0.182	0.011
l	6	7	8	9	10	
R_l	-0.088	-0.006	0.024	0.002	-0.010	

of the series converge rapidly towards zero. The leading coefficient is R_2, which is the only coefficient measurable by IR absorption experiments. Because of the two layer structure of the membrane, the distribution has an additional symmetry, $f(\theta) = f(\theta+\pi/2)$, and therefore all odd Legendre coefficients are expected to vanish. The small, non-vanishing odd coefficients indicate a small asymmetry of the simulated bilayer membrane.

In mean field theories, similar to the Maier-Saupe theory (Chandrasekhar 1992; Maier & Saupe 1958), only the second Legendre polynomial is used as an order parameter. These theories have been used with success to calculate thermodynamic properties in liquid crystals (Chandrasekhar 1992). Smectic-A layers of liquid crystals contain a multi-layer structure similar to lipid bilayers. Therefore the Maier-Saupe theory can be applied to lipid bilayers. Although our simulation has shown that a single order parameter, namely the second Legendre polynomial, can approximate the true distribution of TMs quite well, corrections with higher order Legendre polynomials up to the fourth order might improve mean field models.

5 Conclusions

In this paper, we presented a method to calculate the general dichroic ratio D from MD simulation trajectories. Further, we established a connection between the dichroic ratio R^{ATR}, which is measured in IR-ATR setups, with the general dichroic ratio D, and the order parameter S_{zz}. Considering the different preparation of the experimentally used lipid systems (POPC/POPG mixtures) and the simulated system (pure POPC), the dichroic ratios calculated from the MD simulation were found to be in good agreement with experimental data.

With the aid of the TM model distribution in the lipid coordinate system, which was derived from the MD simulation, it is now possible to determine the mean lipid tilt angles from experimental dichroic ratios. Through computation of the angular distribution of TM orientations, we confirmed the axial rotation symmetry for our model system. Since only small differences between the distributions for the three different orientations in the H–C–H plane, the symmetric, asymmetric and the C–H bond orientation were found, it is possible to compare NMR and IR order parameters[13]. We approximated the asymmetric TM distribution through an expansion in Legendre polynomials. We truncated the series after the second order, because only the second order coefficient can be measured. The approximated distribution is in remarkably good agreement with the original distribution. Therefore, order parameters, which are defined as the second Legendre polynomial of the angular distribution of TM orientations, are a good method to describe the degree of orientation of TM distributions in lipid bilayers. Coefficients of higher order were calculated from the simulation and may be used to improve mean field theories, e.g., Mayer-Saupe theories (Chandrasekhar 1992).

However, a critical remark must be made concerning the error propagation from the experimental R^{ATR} to the order parameters and tilt angle γ. It is experimentally very difficult to accurately measure R^{ATR}. The large errors for R^{ATR} given in Table 2 lead to order parameters and tilt angles covering almost all possible values. Nevertheless, comparison with other experimental IR data ((Brauner *et al.* 1987) in conjunction with the remarks in Appendix B) suggests that the given data are more reliable than the large errors indicate. In this work we compared NMR, ATR, and computer simulation data and found good agreement, which increases confidence in the measurements.

After introducing the concept of a tail director, we performed a detailed structural analysis of tail director orientations. The order parameter of the tail director was calculated and was found to be in good agreement with experimentally derived tail order parameters of lipids other than POPC. The molecular directors were found to be tilted by characteristic tilt angles in both the gel and fluid phase.

With the present work we hope to broaden the basis for further investigations of lipid films and help in the interpretation of experimental results. Future projects include: (i) MD and IR studies of lipid films containing a mixture of different lipids, (ii) the study of the effect of adsorption on a surface with its practical application to bio-sensors, (iii) calculations of IR line shapes from MD data should be possible with the application of Kubo line shape theory (Kubo 1969), and may explain line broadening and line shifts which depend on temperature and phase state of lipid systems.

[13] Note that IR order parameters refer to a lab coordinate system while the NMR order parameter is measured in a local microscopic coordinate system. Since in both cases the molecule directors are oriented parallel to the membrane normal, we found that both distributions can be compared.

Acknowledgement. C. B. is indebted to T. Bayerl for helpful input and for allowing my participation as a member of the E22, biophysics group. C. B. would like to thank M. Bloom and D. Pink for critical remarks on the averaging factor of IR absorption during a discussion in Munich. H. H. would like to thank H. Grubmüller for valuable suggestions, Paul Tavan for helpful discussions, and the SFB 143 of the Deutsche Forschungsgemeinschaft (DFG) for financial support.

The graphs in this paper were prepared with SciPlot (Wesemann 1994) on a NeXTSTEP computer, Figure 3 was produced with MolViewer (Ludtke 1993) on the same computer system.

References

Banko, B., Heller, H. (1991) User Manual for EGO — Release 1.1. [Beckman Institute Technical Report TB-92-07].

Bayerl, T. M., Schmidt, C. F., Sackmann, E. (1988) Kinetics of symmetric and asymmetric phospholipid transfer between small sonicated vesicles studied by high-sensitivity differential scanning calorimetry, NMR, electron microscopy, and dynamic light scattering *Biochemistry* 27:6078–6085.

Bellamy, L. J. (1975) The Infrared Spectra of Complex Molecules, Methuen, London.

Bolterauer, C. (1996) The IR–order parameter and the order tensor: Theory, application to ATR spectroscopy and comparison to the NMR order parameter. Submitted to EBJ.

Brauner, J. W., Mendelsohn, R., Prendergast, F. G. (1987) Attenuated total reflectance fourier transform infrared studies of the interaction of melittin, two fragments of melittin, and δ-hemoysin with phosphatidylcholines studies of the interaction of melittin, two fragments of mellitin, and δ-hemoysin with phosphatidylcholines *Biochemistry* 26:8151–8158.

Brooks, B. R., Bruccoleri, R. E., Olafson, B. D., States, D. J., Swaminathan, S., Karplus, M. (1983) CHARMM: a program for macromolecular energy, minimization, and dynamics calculations *J. Comp. Chem* 4:187–217.

Brünger, A. T. (1988) X-PLOR. The Howard Hughes Medical Institute and Department of Molecular Biophysics and Biochemistry, Yale University, New Haven, CT.

Brünger, A. T. (1990) X-PLOR, Version 2.1. The Howard Hughes Medical Institute and Department of Molecular Biophysics and Biochemistry, Yale University, 260 Whitney Avenue, P.O. Box 6666, New Haven, CT 06511.

Chandrasekhar, S. (1992) Liquid Crystals, Cambridge Uni. Press.

Chia, N. C., Mendelsohn, R. (1992) CH2 wagging modes of unsaturated acyl chains as IR probes of conformational order in methyl alkenoates and phospholipid bilayers *J. Phys. Chem.* 96:10543–10547.

Damodaran, K. V., Merz, Jr., K. M., Gaber, B. P. (1992) Structure and dynamics of the dilauroylphosphatidylethanolamine lipid bilayer *Biochemistry* 31:7656–7664.

Egger, M., Ohnesorge, F., Weisenhorn, A. L., Heyn, S. P., Drake, B., Prater, C. B., Gould, S. A. C., Hansma, P. K., Gaub, H. E. (1990) Wet lipid–protein membranes imaged at submolecular resolution by atomic force microscopy *J. Struct. Biol.* 103:89–94.

Frey, S., Tamm, L. K. (1991) Orientation of melittin in phospholipid bilayers *Biophys. J.* 60:922–930.

Fringeli, U. P., Gunthard, H. H. (1981) Infrared membrane spectroscopy. In: E.Grell (Ed.) *Membrane Spectroscopy*, pp 270–332, Springer–Verlag, Berlin.

Goldstein, H. (1989) Classical mechanics, Addison-Wesley.

Grubmüller, H., Heller, H., Windemuth, A., Schulten, K. (1991) Generalized Verlet algorithm for efficient molecular dynamics simulations with long-range interactions *Molecular Simulation* 6:121–142.

Harrick, N. J., Pre, F. K. D. (1966) *Appl. Optics* 5:1739–1743.

He, K., Ludtke, S. J., Huang, H. W., Andersen, O., Greathouse, D., II, R. E. K. (1994) Closed state of gramicidin channel detected by X-ray in-plane scattering *Biophys. Chem.* 49:83–89.

Heitler, W. (1954) The Quantum Theory of Radiation, V, Oxford Uni. Press.

Heller, H., Grubmüller, H., Schulten, K. (1990) Molecular dynamics simulation on a parallel computer *Molecular Simulation* 5:133–165.

Heller, H., Schaefer, M., Schulten, K. (1993) Molecular dynamics simulation of a bilayer of 200 lipids in the gel and in the liquid crystal phases *J. Phys. Chem.* 97:8343–8360.

Heller, H. (1988) Diploma thesis, Technical University of Munich, Physics Department, T 30, James-Franck-Street, D-8046 Garching / Munich.

Heller, H. (1993) Simulation einer Lipidmembran auf einem Parallelrechner. Doctoral dissertation, Technical University of Munich, Germany.

Hübner, W., Mantsch, H. H. (1991) Orientation of specifically ^{13}C=O labeled phosphatidylcholine multilayers from polarized attenuated total reflection FT-IR spectroscopy *Biophys. J.* 59:1261–1272.

König, S., Pfeiffer, W., Bayerl, T., Richter, D., Sackmann, E. (1992) Molecular dynamics of lipid bilayers studied by incoherent quasi-elastic neutron scattering *J. Phys. II France* 2:1589–1615.

Kubo, R. (1969) *Adv. Chem. Phys.* 15:101.

Ludtke, S. (1993) MolViewer. Physics Dept., Rice University, Houston, TX 77251-1892, e-mail: stevel@alumni.caltech.edu. Version 0.92 β.

Maier, W., Saupe, A. (1958) *Z. Naturforsch* 13a:564.

Raine, A. R. C. (1990) Molecular dynamics simulation of proteins on an array of transputers. In: Pritchard, D. J., Scott, C. J. (Eds.) *Applications of Transputers 2., Proccedings of the Second International Conference on Applications of Transputers*, pp 272–279, Amsterdam, Netherlands, IOS Press.

Ryckaert, J.-P., Ciccotti, G., Berendsen, H. J. C. (1977) Numerical integration of the cartesian equations of motion of a system with constraints: Molecular dynamics of n-alkanes *J. Comp. Phys.* 23:327–341.

Schachtenschneider, J. H., Snyder, R. G. (1962) Vibrational analysis of the n-paraffins-ii. normal co-ordinate calcualtion *Spectrochim. Acta* 19:117–168.

Seelig, J., Macdonald, P. M. (1987) Phospholipids and proteins in biological membranes. ^{2}H NMR as a method to study structure, dynamics, and interactions *Acc. Chem. Res.* 20:221–228.

Seelig, J., Seelig, A. (1980) Lipid conformation in model membranes and biological membranes *Quart. Rev. Biophys.* 13:19–61.

Seelig, J. (1977) Deuterium magnetic resonance: Theory and application to lipid membranes *Quart. Rev. Biophys.* 10:353–418.

Sinha, A. B., Schulten, K., Heller, H. (1994) Performance analysis of a parallel molecular dynamics program *Comput. Phys. Commun.* 78:265–278.

Small, D. M. (1986) The Physical Chemistry of Lipids, Plenum Publishing Corp., New York.

Snyder, R. G., Schachtenschneider, J. H. (1963) Vibrational analysis of n-paraffins-i. *Spectrochim. Acta* 19:85–117.

Tuchtenhagen, J., Ziegler, W., Blume, A. (1994) Acyl chain conformational ordering in liquid-crystalline bilayers: comparative FT-IR and 2H-NMR studies of phospolipids differing in headgroup structure and chain length *Eur. Biophys. J.* 23:323–335.

Verlet, L. (1967) Computer “experiments” on classical fluids. I. Thermodynamical properties of Lennard-Jones molecules *Phys. Rev.* 159:98–103.

Wesemann, M. (1994) SciPlot. Schillerstr. 73, 10627 Berlin, Germany, e-mail: mike@calamity.rz-berlin.mpg.de (NeXTMail preferred). Version 3.99.

Zaccai, G., Büldt, G., Seelig, A., Seelig, J. (1979) Neutron diffraction studies on phosphatidylcholine model membranes. II. chain conformation and segmental disorder *J. Mol. Biol.* 134:693–706.

A Directional Cosine

To generate the azimuthal or directional cosine in direction (α, β) we transform a set of unit spherical coordinates $\mathbf{u}_{spherical}$

$$\mathbf{u}_{spherical}(\theta, \varphi) = \begin{pmatrix} cos(\varphi)\ sin(\theta) \\ sin(\varphi)\ sin(\theta) \\ cos(\theta) \end{pmatrix} \quad . \tag{22}$$

The z-component can be transformed to the directional cosine $z = cos(\theta) \to Z$, by making use of the well known rotation matrix $\mathbf{A}(\phi, \theta, \psi) = D_z(\psi) D_x(\theta) D_z(\phi)$ (Goldstein 1989). Using the Euler angles $\psi = \pi/2 - \xi, \theta = \beta, \phi = \pi/2 + \alpha$, the transformed z-component reads

$$Z(\alpha, \beta, \theta, \varphi) = [\mathbf{A}(\xi, \beta, \alpha)\ \mathbf{u}_{sherical}(\theta, \varphi)]_z \quad , \tag{23}$$

thus gives Eq. (3)

$$\begin{aligned} Z(\alpha, \beta, \theta, \varphi) = {} & cos(\alpha)\ sin(\beta)\ cos(\varphi)\ sin(\theta)\ + \\ & sin(\alpha)\ sin(\beta)\ sin(\varphi)\ sin(\theta) + \\ & cos(\beta)\ cos(\theta) \quad . \end{aligned} \tag{24}$$

B Brauner

Because we do not find the refraction index of the bulk medium, $n_3 = 1$, used in (Brauner *et al.* 1987) reasonable, we recalculated the evanescent fields **E**, the dichroic ratio D, and the order parameter S_{zz} for different refraction indices n_3 of the bulk medium.

Table 5. Effect of the refraction index n_3 of the bulk media: Recalculated evanescent fields **E**, dichroic values D and order parameters S_{zz}^{IR} of POPC in the fluid phase are derived from the experimental dichroic ratio $R^{ATR} = 1.18$ given by Brauner et. al. (Brauner *et al.* 1987). The experimental values were obtained from the asymmetric CH_2 line. Eqs. (14) and (17) were used to recalculate the values.

n_3	E_x^2	E_y^2	E_z^2	β	R^{ATR}	D	S_{zz}^{IR}
1.33	1.969	2.249	1.840	46.0	1.18	0.372	-0.264
1.20	1.980	2.198	1.165	52.5	1.18	0.526	-0.188
1.00	1.991	2.133	0.529	62.7	1.18	0.994	-0.002

This article was processed by the author using the LaTeX style file *cljour2* from Springer-Verlag.